Development of Fe_2O_3-Based Catalysts of Different Geometries for Environmental Catalysis

L. A. ISUPOVA, V. A. SADYKOV, S. V. TSYBULYA, G. S. LITVAK, G. N. KRYUKOVA, E. B. BURGINA and A.V. GOLOVIN

G. K. Boreskov Institute of Catalysis, Siberian Branch of the Russian Academy of Sciences,
Pr. Akademika Lavrentyeva 5, Novosibirsk 630090 (Russia)

E-mail: isupova@catalysis.nsk.su

Abstract

X-ray, TA, IRS, TEM and BET techniques were used to study the effect of mechanical treatment in a centrifugal planetary ball mill EI 2×150 and in a continuously operating vibration ball mill VCM-25 on physicochemical properties of powdered iron oxide of different prehistory, as well as on the properties of produced granulated supports and catalysts. The influence of structure-forming additives and electrolyte was discussed. The influence of the method used for introduction of the active component on the catalyst properties for complete oxidation of butane and CO was established.

INTRODUCTION

Iron oxide, α-Fe_2O_3, is an abundant inexpensive chemical, which is stable in reaction media. For these reasons, it seems very attractive for development of complete oxidation catalysts to abate industrial emissions of CH_x, CO, NO_x. Relatively high strength of the Fe–O bond makes it more suitable for high temperature (800–900 °C) catalytic oxidation processes. When modified with noble metals (Pt, Pd, Au, Ag, *etc.*) or active oxides such as CuO, Co_3O_4, MnO_x, $LaMnO_3$, it can also be used for low temperature processes [1–3]. The vital importance of environmental protection imposes severe restrictions on the amount and composition of wastewater produced during catalysts preparation. Therefore, dry methods including the so-called kneading technology are now of a special interest. Since extrudability of the feedstock – powdered iron oxides – is insufficient, it seems reasonable to include stages of mechanical activation and/or binding, similar to those used before for preparation of CuO and Co_3O_4 monolith catalysts [4, 5], in the technology of these catalysts preparation. These expedients make it possible not only to improve rheological characteristics of the pastes and to introduce thermostabilizing additivities but also to prepare catalysts of the required shape. The now preferable shape is a honeycomb monolith to provide considerably lower pressure drop and a better performance of the catalytic process [6, 7].

The aim of the present study is to develop complete oxidation iron oxide-based catalysts of different shapes, including monoliths, prepared by the kneading technology. Mechanical activation of Fe_2O_3 powders is used to impart appropriate rheological properties to the plastic pastes based on iron oxide. Besides, binders comprising Al_2O_3 and various electrolytes are added. Active components are either introduced by wet impregnation of the support or added to the paste.

EXPERIMENTAL

The initial compounds were iron oxides prepared by different procedures. Fe_2O_3 of special purity grade (s.p.g.) was prepared by thermal decomposition of ammonium oxalatoferrite $(NH_4)_3[Fe(C_2O_4)_3] \cdot 3H_2O$ (s.p.g.) followed by calcination in air at 500 °C for 24 h. Fe_2O_3-(CO_3) was prepared by calcining iron carbonate at 500–600 °C; the iron carbonate was precipitated from the solution of iron sulfate (pH 7–8) under the action of ammonium carbonate (co-precipitation) according to Technical Specifications 113–03–317–86 at the Kemerovo Azot Co. Fe_2O_3-(Cl) was prepared from $FeCl_2$ solution using a thermospraying column at *ca.* 800 °C according to Technical Specifications 14–15–228–90 at the Novokuznetsk Metallurgical Plant. The other compounds were aluminium hydroxide prepared by thermochemical activation (Technical Specifications 6–68–109–89, Novosibirsk), CrO_3, CuO, Co_3O_4, $Cu(NO_3)_2$, $Al(OH)_3$, HNO_3, CH_3COOH and NH_4OH (chemical purity grade). Aluminium oxinitrate containing 50 to 100 g/l of Al_2O_3 was prepared by neutralization of aluminium nitrate solution at 80 °C to reach pH 3. Preparation details and characteristics of mixed perovskite-containing oxide $LnMnO_3$ are given elsewhere [7].

Mechanical treatment (MT) was conducted in argon using a centrifugal planetary ball mill EI 2×150 with cylinders and corundum-based milling balls of 5–8 mm diameter at acceleration of *ca.* 40 g and varied MT time. MT in air was conducted using a continuously working mill VCM-25; the mill was made of steel and filled with 6 mm steel balls by 50 % (200 balls) of its volume. The oxide to be activated was fed at the rate of 6 kg/h; the number of oxide passages through the mill was varied.

Catalysts were prepared by mixing initial or MT oxides with water, solutions of nitric, acetic or chromic acids, aluminium hydroxide or oxinitrate until the plastic paste was formed. The paste was extruded through differently shaped dies. Extruded granules were dried in air then in a drying oven at 110 °C and calcined in air at 500 °C. The active component was introduced into the catalyst by impregnating the prepared granules with saturated solutions of copper or cobalt nitrates or by adding powdered oxides (CuO, Co_3O_4, $LnMnO_3$) into the paste to be extruded. The percentage of the active oxide was 10 to 14 %.

Catalysts and initial powders were characterized by X-ray, IRS, TEM, TA, BET and high-pressure mercury porosimetry techniques. Determined characteristics were powder magnetization (using Faraday's balance [8]), aggregate size (by Coulter's method [9]) and crushing strength of granules. To identify the size of primary (more strong) and secondary (less strong) aggregates, two versions of measurements were used, *i. e.* powders were subjected or not subjected to preliminary ultrasonic (US) dispersing in isotone. Catalytic activity in oxidation of butane and CO was studied using flow circulation installations for catalyst fractions and granules. Concentration of butane in the air mixture was 0.2 %, initial CO concentration 1 %, gas flow rates 10 l/h, circulation rate 1000 l/h, water was not frozen.

RESULTS AND DISCUSSION

Influence of preparation method on physical and chemical properties of Fe_2O_3 oxides

Physicochemical properties and reactivity, including catalytic activity, of oxides depend largely on the preparation conditions that affect their specific surface area, morphology, microstructure, impurity composition and defects [10–12]. That is why different iron oxide samples have been used for the present study. These are Fe_2O_3-(Cl) ($S_{sp} \approx 6$ m^2/g) prepared by decomposition of $FeCl_2$, Fe_2O_3-(CO_3) ($S_{sp} \approx$ 35 m^2/g) prepared by decomposition of iron carbonate/bicarbonate, Fe_2O_3-(s.p.g.) ($S_{sp} \approx$ 12 m^2/g) prepared by decomposition of ammonium oxalatoferrite. The phase composition corresponds to α-Fe_2O_3 for Fe_2O_3-(Cl) and Fe_2O_3-(s.p.g.) and to a mixture of α- and γ-modification of Fe_2O_3 for Fe_2O_3-(CO_3). From TEM data (Fig. 1), micron size and rounded edges are characteristic of the iron oxide particles. The particle shape varies from round (more pronounced for the s.p.g. sample) to oblong (for the carbonate and chloride samples).

The Coulter data show that all the initial samples are aggregated (the aggregates vary in size in the range of 10 to 20 μm) and do not form well-extrudable plastic pastes upon mixing with water. When extruded, the pastes are stratified, and the produced granules are of low strength. MT can be used to control the

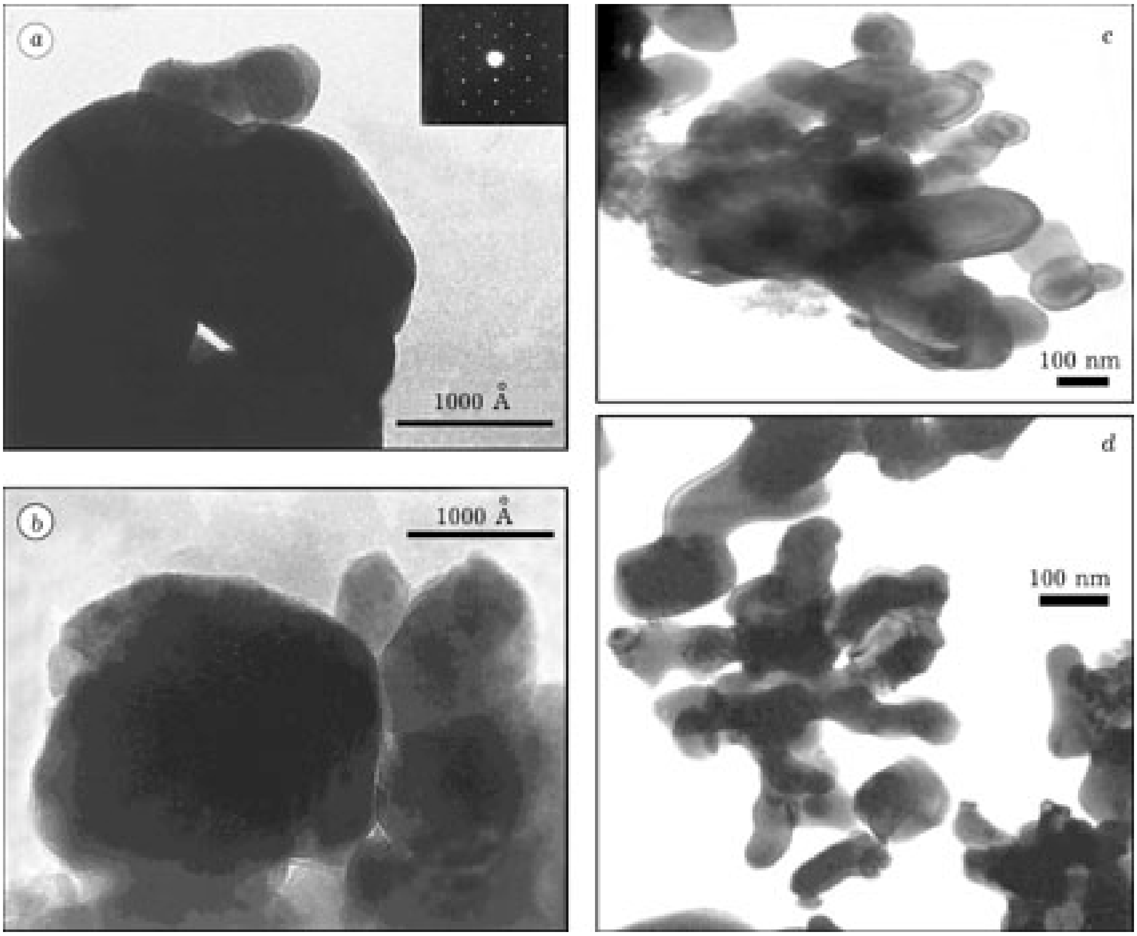

Fig. 1. TEM data for Fe_2O_3 samples *vs.* preparation method (*a, c, d*) and after mechanical treatment in EI ball mill for 15 min (*b*): *a* and *b* – Fe_2O_3-(s.p.g.); *c* – Fe_2O_3-(CO_3); *d* – Fe_2O_3-(Cl).

extrudability. The data on the influence of MT on iron oxide properties are presented below.

Influence of mechanical treatment on the physical and chemical properties of Fe_2O_3

The influence of MT time in argon in an EI 2×150 mill on the physicochemical properties of Fe_2O_3-(s.p.g.) has been thoroughly studied before [13]. From the Coulter data, mechanical activation in the EI 2×150 mill results in a decrease in the average aggregate size from *ca.* 14 to *ca.* 9 μm (without US dispersing) or from 12 to 8 μm (after US dispersing) that indicates the sufficient strength of the primary aggregates and practically full MT destruction of the secondary aggregates. It is shown that the physicochemical properties change noticeably upon not shorter than 10 min MT. At short MT times (less than 5 min), no considerable change is detected by XRA, TA, IRS and TEM.

For example, TEM studies demonstrate that the rounded shape and particle size is preserved even after 15 min MT (see Fig. 1, *b*). Peeling of fine (80–100 Å) layers from coarse particles (*ca.* 1000 Å) to form split edges is observed [13].

From the X-ray data, the coherent scattering region (CSR) decreases from *ca.* 450 Å for the initial oxide to *ca.* 200 Å for the oxide subjected to 15 min MT. The expected surface area is 40–60 m^2/g for particles of this size that is 2–3 times as high as that measured by BET (14–21 m^2/g). Hence, the particles may be polycrystalline and/or contain intergrain boundaries.

It is also established that MT of hematite results in high density of surface and/or bulk point defects. The defects, when contact atmospheric air, produce surface hydroxides and carbonates. Similar phenomena have been observed earlier [14] during mechani-

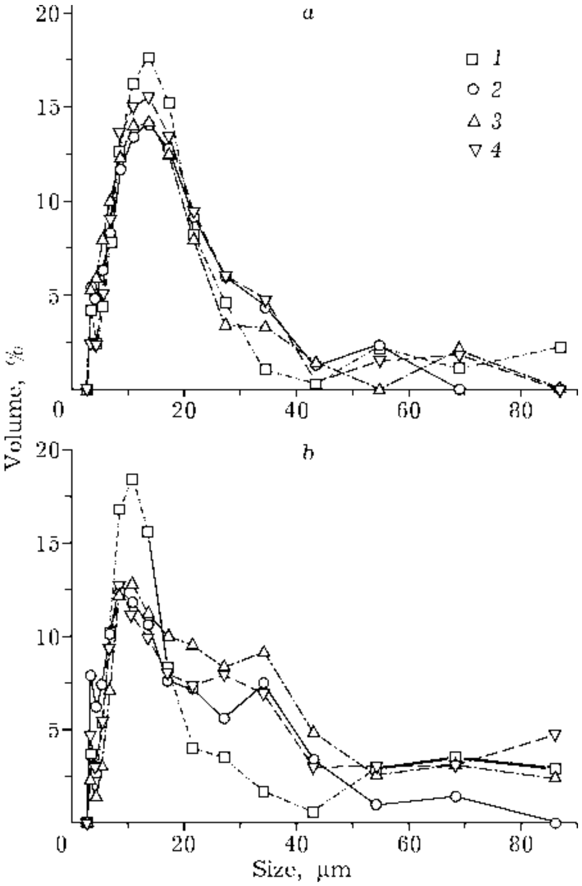

Fig. 2. Aggregates size according to Coulter data (without dispersion) *vs.* mechanical treatment (passing number n = 0 (*1*), 1 (*2*), 3 (*3*), 5 (*4*) top-down) in VCM-25 ball mill for Fe_2O_3-(CO_3) (*a*) and Fe_2O_3-(s.p.g.) (*b*).

cal treatment of copper oxide in air for 1–3 min.

Neither specific surface area nor primary aggregate size (determined at sample dispersing before measurements) is observed during MT of all samples in air in VCM-25 mill (Fig. 2, Table 1). However, the secondary aggregates of Fe_2O_3-(s.p.g.) do not decrease but increase in size that indicates aggregation of iron oxide particles during MT in air. The aggregation may result either from more considerable level of surface hydration during MT in air or from sample magnetization due to rubbing against the mill pieces.

The careful comparative X-ray studies of the influence of MT in VCM on the phase composition, CSR and structural parameters of Fe_2O_3-(s.p.g.) revealed no detectable MT-induced changes in these parameters, unlike the ones described above. Changes in the IR spectra also are negligible.

At the same time, it is shown by thermal analysis in air that mechanical treatment of Fe_2O_3-(s.p.g.) and Fe_2O_3-(CO_3) in the VCM mill gives rise to an exoeffect at 335 °C accompanied with weight loss. The thermal effects increase in intensity with increasing mechanical impact (number of passages through the mill); they are more pronounced with Fe_2O_3-(CO_3) possessing a higher specific surface area (Fig. 3). If keep in mind the processes of reduction and hydration of oxides in the course of MT, one cannot exclude that the exoeffect observed at this temperature is the result of several processes, *i. e.* endothermic decomposition of hydrated disordered/amorphized layer formed during MT and subsequent exothermic processes of oxidation and crystallization of the disordered/amorphized reduced oxide formed upon decomposition of the hydrated layer. The

TABLE 1

Particle size and specific surface of Fe_2O_3 powder samples *vs.* mechanical treatment in VCM-25 ball mill

Sample	Passing number, n	S_{sp}, m^2/g	Aggregate size (without US dispersion)	Aggregate size (US dispersion 2 min)
Fe_2O_3-(s.p.g.)	0	12	14	9
	1	14	13	11
	3	14	18	10
	5	13	17	10
Fe_2O_3-(CO_3)	0	31	14	10
	1	33	13	13
	3	33	12	10
	5	34	14	10
Fe_2O_3-(Cl)	0	5.2	17	12

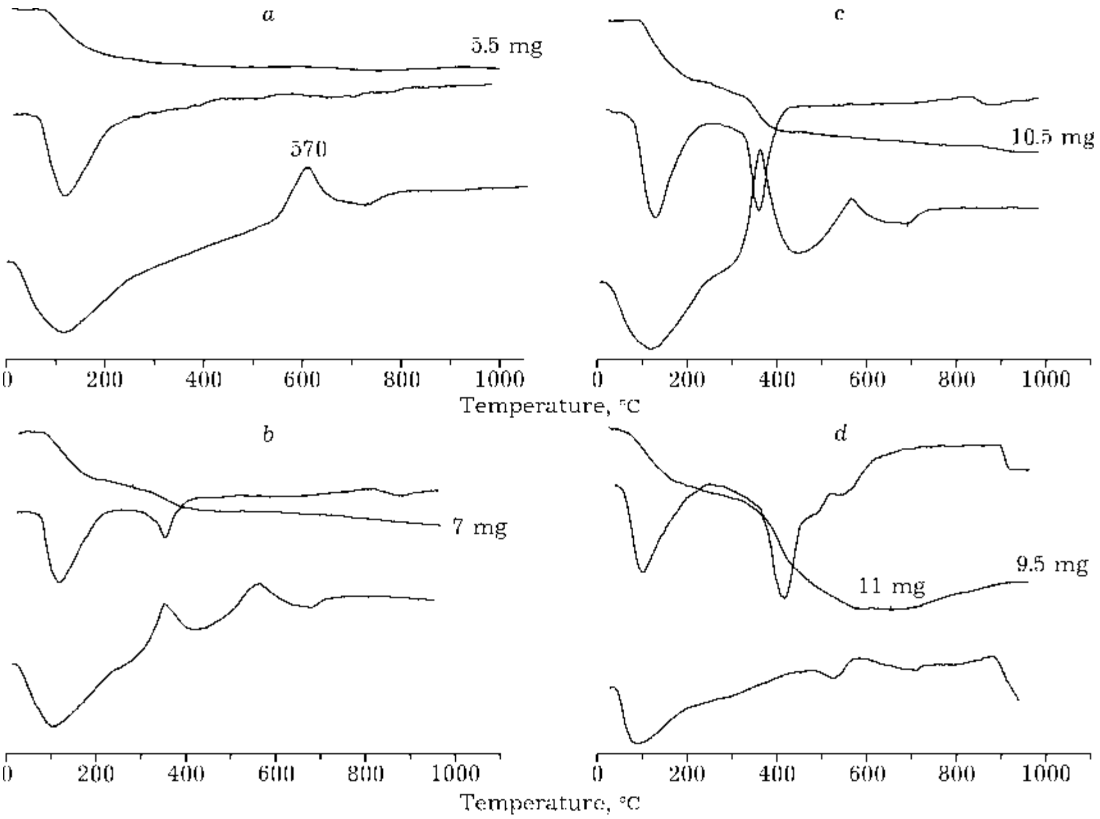

Fig. 3. TA data in air and in He for Fe_2O_3-(CO_3) *vs.* mechanical treatment (passing number n = 0 (*a*), 3 (*b*), 5 (Air) (*c*) and 5 (He) (*d*) top-down). Samples mass 500 mg, heating rate 10 °C/min. Mass loss is indicated in figures.

amount of the reduced hydrated layer produced in 5 passages during MT of Fe_2O_3-(CO_3) assumed to be comprised of $Fe(OH)_2$ is calculated based on TA data on weight loss and equation

$$2Fe(OH)_2 + 1/2O_2 = Fe_2O_3 + 2H_2O$$

According to the calculations, the hydroxide is formed in amount of *ca.* 7.2 % of, or 4 10^{-4} mol in the given weighed sample, during MT. If the assumption about the exoeffect nature is valid, then more considerable weight loss and lower exoeffect should be expected after heating the MT sample in inert atmosphere because the process of sample oxidation is excluded.

The data obtained show indeed that heating in flowing helium is accompanied by more considerable weight loss at practically undetectable exoeffect (see Fig. 3). The same value, *ca.* 7 % on the basis of $Fe(OH)_2$, is obtained by calculation of the amount of the reduced hydrated layer from the data on weight loss by equation

$$Fe(OH)_2 = FeO + H_2O$$

The exoeffect is not observed in DTA curves recorded in flowing helium. Therefore, decomposition of the disordered hydrated layer either proceeds without heat effect or is compensated by the crystallization exoeffect that allows the TA-detected exoeffect in air to be attributed to oxidation of reduced Fe^{2+} cations to Fe^{3+}. Quantitative analysis of the observed exoeffect (after 5 passages) based on TA data for reference compounds gives the value of *ca.* 100 J/g of sample that practically coincides with the heat effect of the reaction of oxidation of FeO into Fe_2O_3: ~290 kJ/mol Fe_2O_3 or ~580 kJ/mol O_2 or ~130–140 kcal/mol O_2.

The data obtained allow the conclusion about formation of reduced hydrated iron cations in amount of up to 7 % (on the basis of $Fe(OH)_2$) during MT of Fe_2O_3-(CO_3) in VCM and up to 2 % during MT of Fe_2O_3-(s.p.g.). The latter amount coincides with the one calculated for Fe_2O_3-(s.p.g.) subjected to 5 min MT in ceramic drums [13]. Since a noticeable exoeffect at 270 °C, like that appeared at long activation

TABLE 2

Magnetic properties of α-Fe_2O_3-(s.p.g.) powders *vs.* mechanical treatment

Sample and its MT	Magnetization, Gs cm^3/g		γ-Fe_2O_3, %
	3700 Oe	7400 Oe	
Fe_2O_3-(s.p.g.), $n = 0$	0.44	0.56	0.3
Fe_2O_3-(s.p.g.), $n = 1$	2.29	2.61	2
Fe_2O_3-(s.p.g.), $n = 3$	2.41	2.63	–
Fe_2O_3-(s.p.g.), $n = 5$	3.36	2.58	–
Fe_2O_3-(s.p.g.), MT 15 min in Ar	0.30	0.39	0.23
Fe_2O_3 (goethite, 700 °C)	0.07	0.14	–

times (longer than 10 min [13]), as well as considerable spectral or structural changes are not observed in this case, the mechanical impact in VCM during 5 passages is considered corresponding to the 5 min MT in the EI mill. It is hardly possible to compare resuts for different mills more precisely because the processes of formation of the reduced hydrated layer on the iron oxide surface during MT may be affected additionally by the mill material (in the case of milling by metal balls) to result in addition reduction of iron oxide by reaction

$$Fe_2O_3 + Fe \rightarrow Fe_3O_4$$

An increase in magnetization is supported by magnetic measurement of the samples (Table 2). It is shown that the calculated content of the ferromagnetic impurity in MT samples equals *ca.* 2 % in VCM, even after 1 passage, white being not higher than *ca.* 0.23 % in ceramic drums.

In agreement with Schukin and Rebinder concepts, hydration of MT sample surface in VCM results in better extrubabilty and higher granule strength. However, it is not appropriate to boost VCM mechanical impact by increasing the passage number in order to increase the degree of surface hydration. If do so, powder magnetization and secondary aggregate size increase that may cause the so-called powder "hanging" or a considerable decrease in the rate of powder discharging from the mill.

Influence of the mechanical treatment on the Fe_2O_3 granule properties

It is discovered that extrudable unstratified plastic pastes can be formed from all Fe_2O_3 powders subjected to mechanochemical treatment (even with pure water free of acid), but not from untreated powders. As a result of the mechanochemical treatment, the aggregates and crystallites decrease in size, the surface microstructure and chemistry changes (hydration of the surface). The surface becomes more wettable at lower paste humidity, pores decrease in size and volume in the calcined iron oxide granules, while the crushing strength increases (Table 3).

Examination of reasons for increasing granule strength allows the suggestion that at minor MT impacts the granules are mainly strengthened due to an increase in the strength of unit contacts neither average pore volume nor average pore radius change and, if follow the Schukin–Rebinder model, the number of contacts does not change. Strengthening of unit contact in MT samples is accounted for by an increase in the contact area between particles. It should be noticed that the volume of coarse pores in sample Fe_2O_3-(CO_3), even after 5 passages through VCM, remains practically the same as that in the initial sample at somewhat decreased volume of fine pores (Fig. 4, *a*, curves *1* and *3*). Calcination of the granules at 500 °C results in practically equal decrease in the proportion of coarse pores and total porosity (see Fig. 4, *a*, curves *1* and *3*). Therefore, it is reasonable to conclude that Fe_2O_3-(CO_3) granules are mainly strengthened due to strengthening of unit contacts after mechanical treatment but due to an increase in the contact number and strength after calcination.

Mechanical treatment of Fe_2O_3-(s.p.g.) can also result in an increase in the number of contacts because both total pore volume and

TABLE 3

Properties of Fe_2O_3 granules (∅ 4 mm) calcined at 500 °C *vs.* mechanical treatment (samples No. 1–4 prepared from Fe_2O_3-(s.p.g.); samples No. 5–8 prepared from Fe_2O_3-(CO_3))

Sample No.	Passing number n in VCM-25	Paste humidity, %	S_{sp}, m^2/g	P_o, kg/cm^2	V, cm^3/g
		α-Fe_2O_3-(s.p.g.), S_{sp} = 12 m^2/g			
1	0	37.5	12	10	0.53
2	1	31.5	11	25	–
3	3	20.6	9.4	34	–
4	5	19.4	9.8	37	0.21
		α + γ-Fe_2O_3-(CO_3), S_{sp} = 34 m^2/g			
5	0	33	27	14	0.45
6	1	32	24	16	0.45
7	3	30.6	24	22	–
8	5	28.6	20	20	0.38

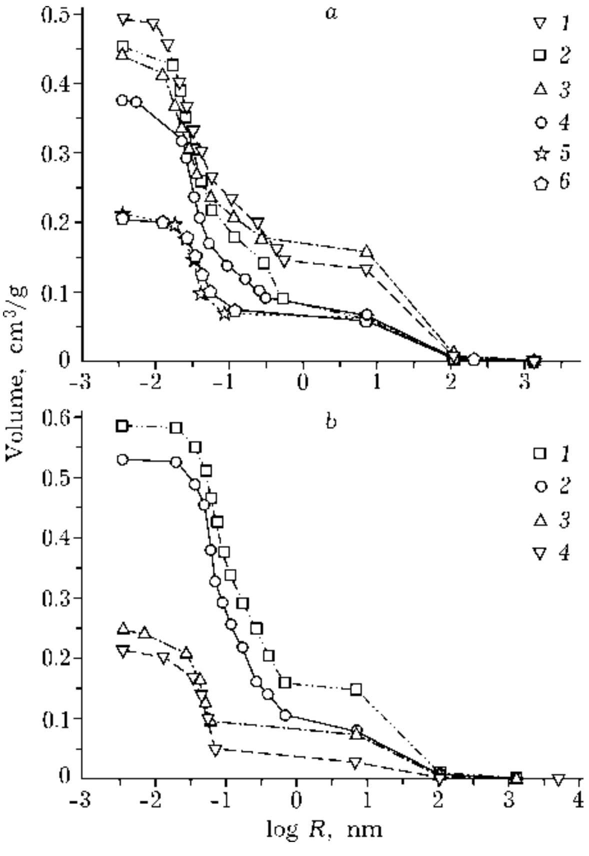

Fig. 4. Pore structure of Fe_2O_3-(CO_3)(*a*) and Fe_2O_3-(s.p.g.) (*b*) *vs.* preparation conditions: *1, 3* – granules were dried at 110 °C (electrolyte water); *2, 4–6* – granules were calcined at 500 °C (*2, 4* – electrolyte water, *5, 6* – electrolyte chromic acid); *1, 2, 5* – MT didn't used; *3, 4, 6* – powders were treated in VCM-25, n = 5.

the volume of coarse pores decrease in the dried samples (see Fig. 4, *b*, curves *1* and *3*). Calcination at 500 °C causes mainly a decrease in the proportion of coarse pores, *i. e.* an increase in the number of contacts (see Fig. 4, *b*, curves *1* and *2–4*).

The data obtained indicate different reasons for strengthening of granules of different oxides subjected to MT. Granules of Fe_2O_3-(CO_3) are predominantly strengthened due to strengthening of unit contacts at only minor decrease in the paste humidity (see Table 3). In the case of Fe_2O_3-(s.p.g.), the main reason is an increase in the number of contacts, probably due to more considerable decrease in the paste humidity during extrusion compared to that of the initial oxide (see Table 3). It cannot be excluded that the humidity decreases during extrusion because of considerable decrease in the proportion of fine pores in the course of mechanical treatment of Fe_2O_3-(s.p.g.) powder.

The different nature of the MT influence on porous structure of oxides Fe_2O_3-(CO_3) and Fe_2O_3-(s.p.g.) may be the result of different morphology of the initial oxides and, in particular, different nature of fine pores in the oxides. For example, these are intercrystallite pores caused by the close crystallite packing in the case of Fe_2O_3-(CO_3) but intracrystallite pores in the case of Fe_2O_3-(s.p.g.). Conditions

TABLE 4

Properties of Fe_2O_3 granules (∅ 4 mm) calcined at 500 °C *vs.* binder and electrolyte nature

Sample No.	Binder/electrolyte	Passing number n in VCM-25	Paste humidity, %	S_{sp}, m^2/g	P_o, kg/cm^2	V, cm^3/g
α-Fe_2O_3-(s.p.g.), 12 m^2/g						
1	H_2O	0	37.5	12	10	0.53
2	ONA	0	33.3	18	15	0.50
$\alpha + \gamma$-Fe_2O_3-(CO_3), 34 m^2/g						
3	H_2O	0	33	27	14	0.45
4	ONA	0	33.3	32	15	0.43
5	HATCA(10 %)	0	24	44	24	–
6	HATCA (10 %)	3	18	55	53	0.3
7	H_2CrO_4	0	25	23	44	0.21
8	H_2CrO_4	5	25	24	56	0.21
α-Fe_2O_3-(Cl), 5 m^2/g						
9	H_2O	0	2.3	4.5	Not formed	–
10	HATCA (10 %)	0	20.3	29	20	0.25
11	HATCA (30 %)	0	27.5	61	29	–
12	H_2CrO_4	0	25	7.7	21	0.27
13	H_2CrO_4	1 (10)*	14	9.3	26	
14	H_2CrO_4	1 (20)*	15	8.6	22	

*In brackets ball diameter is indicated.

of preparation of these oxides may cause the difference. At low decomposition temperatures, nuclei of the new phase are few in number and the diffusion mobility of cations is low. Therefore, the formed particles comprise inner micropores, sometimes pseudomorphous, which usually are easy to destruct. At high decomposition temperatures, a large number of nuclei are formed. The diffusive mobility of cations is higher that results in formation of non-porous crystallites, which are sintered to produce strong enough microporous particles.

Influence of binder and electrolyte nature on the granule properties

Plastic pastes and granules can be prepared by adding alumina-based binders (5–20 %) or chromic acid without mechanochemical treatment. Table 4 shows data on application of binders – aluminium oxinitrate, aluminum hydroxide prepared by thermochemical activation technology (HATCA) and chromic acid – for preparation of granules. With Fe_2O_3-(CO_3) and Fe_2O_3-(Cl), the granules are much stronger when chromic acid is used in place of water (samples No. 3, 7, 9 and 12 in Table 4).

Addition of chromic acid instead of water to initial Fe_2O_3-(CO_3) results in a considerable decrease in the humidity of the prepared paste (see Table 4). No additional change in the paste humidity but somewhat higher granule strength is observed upon mechanochemical pretreatment of the oxide (see Table 4). Therefore, the strengthening of granules observed upon electrolyte replacement may be accounted for by an increase in the number of contacts because the humidity decrease is accompanied by a decrease in the total pore volume (see Fig. 4, *a*, curves *2* and *5*, *4* and *6*). One cannot exclude that the strength of interparticle contact is increased as well, since the pore size distribution is identical for samples No. 5 and 6.

At the same time, paste humidity does not change upon addition of chromic acid instead of water to Fe_2O_3-(Cl) but the humidity decreases after MT (see Table 4). The paste humidity does not change during extrusion of this oxide with various electrolytes (see Table 4, samples No. 9 and 12) that allows the observed strengthening of granules prepared with chromic acid to be mainly accounted for by strengthening of unit contacts.

Introduction of a weak acidic electrolyte (for example, AON solution at pH 4) into samples of Fe_2O_3-(CO_3) and Fe_2O_3-(s.p.g.) does not result in considerable change in the extruded paste humidity or porous structure (the curve is identical to curve *2* in Fig. 4, *b*) and granule strength (see Table 4, samples No. 1–4) at the alumina content 3 –5 % in the calcined granules.

An increase in the concentration of Al_2O_3 binder (HATCA) causes granule strengthening even in the neutral medium (without acid electrolyte) (see Table 4, samples No. 3–5 and 9–11). In this case MT allows considerable additional strengthening of the granules (samples No. 5 and 6 in Table 4).

Thus, the influence of MT on the strength and porous structure of various oxides is the same in the cases of the acidic electrolyte and water, although the effect of MT on the strength is less pronounced against the more considerable effect of acidic electrolyte.

The data obtained show that application of mechanochemical treatment, electrolyte and Al_2O_3 binder makes it possible to control the extrudability and strength of iron oxide granules over wide ranges. The reasons for strengthening depend on prehistory of the initial iron oxide and the preparation procedure. Properties of plastic pastes can be optimized by applying mechanochemical activation of iron oxide, varying the amount of a binder and electrolytes nature and concentration in order to produce monolithic carriers/catalysts and to control their strength and pore structure. For example, hexagonal micromonoliths with triangle channels and walls of 1 mm thickness can be prepared from all kinds of iron oxide with added chromic acid. Introduction of HATCA and solutions of nitric or acetic acid also allow monoliths to be prepared, the minimal concentration of Al_2O_3 being *ca.* 5 %.

Influence of active oxide on the catalyst properties

The method of introduction of active components into Fe_2O_3 supports is found to affect the catalytic activity, porous structure depending on the nature of iron oxide. Impregnation of MT Fe_2O_3-(CO_3) support or addition of the active component at the stage of kneading results in a considerable decrease in the total volume of proportion of coarse pores in the catalyst granules in comparison to those in the initial support (Fig. 5, *a*). If the Fe_2O_3-(Cl) support prepared without MT is impregnated, the porous structure of the catalyst is practically identical to that of the support (see Fig. 5, *b*).

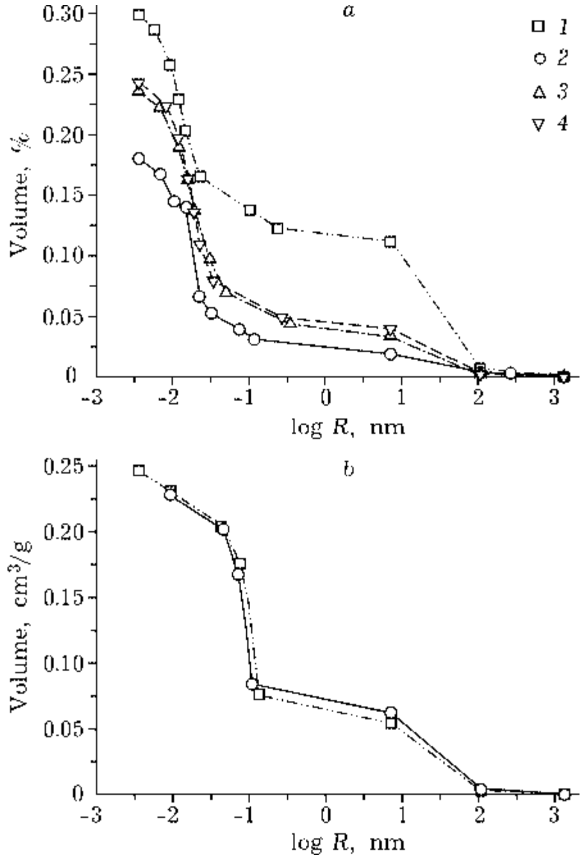

Fig. 5. Catalysts pore structure *vs.* active oxide addition method for different Fe_2O_3 oxides: *a* – Fe_2O_3-(CO_3) after mechanical treatment, *n* = 3; *b* – Fe_2O_3-(Cl), *n* = 0; *1* – carrier prepared from Fe_2O_3 + 10 % HATCA, electrolyte water; *2* – catalyst with ~12 % CuO, prepared after carrier (*1*) nitrate impregnation; *3, 4* – catalysts with ~12 % CuO or Co_3O_4, respectively, prepared kneading technology.

Table 5 shows data on catalytic activity to oxidation of butane obtained with copper oxide and cobalt oxide catalysts prepared by impregnation or kneading (samples No. 1–4). The low catalytic activity of “impregnated” catalysts can be accounted for by modification of the active component with Fe and Al due to dissolution of the support during impregnation with saturated acidic nitrate solutions [15].

TABLE 5

Catalysts properties (granules ∅ 4 mm calcined at 500 °C)

Sample No.	Method of active oxide adding	Active oxide content, %	Powders content during kneading and MT	S_{sp}, m^2/g	P_o, kg/cm^2	V, cm^3/g	W 10^2, cm^3 butane/(g s) at 400 °C	
							particles	granules
1	Kneading	12.5 % CuO	(Fe_2O_3-(CO_3) + 10 % HATCA), n = 3, + active oxide	33	48	0.24	2.24	0.46
2	»	12.5 % Co_3O_4		38	54	0.24	5.75	0.74
3	Impregnation	10.5 % CuO	(Fe_2O_3-(CO_3) + 10 % HATCA), n = 3	35	53	0.18	0.98	0.27
4	»	14.8 % Co_3O_4		34	24	0.24	1.55	0.62
5	IC-12-1*	26 % CuO	γ-Al_2O_3**	–	36	–	1.1	0.47
6	ICT-12-6*	26 % CuO	γ-Al_2O_3**	–	11	–	1.9	0.26
7	MPB-PC*	5 % CuO + 10 % Co_3O_4	α-Al_2O_3**	–	100	–	0.25	0.21
8	Kneading	19 % Cr_2O_3	Fe_2O_3-(CO_3), n = 5	24	56	0.21	9.78	1.5
9	»	19 % Cr_2O_3	Fe_2O_3-(CO_3), n = 0	23	44	0.21	7.97	1.23
10	MTC*	12 % Cr_2O_3	Fe_2O_3-(CO_3), n = 0	25	25	0.31	–	1.06
11	Kneading	10 % $LnMnO_3$	(Fe_2O_3-(Cl) + 30 % HATCA), n = 0	55	29	0.26	–	0.5

*For comparison.

**Carrier.

In the kneading procedure, the acidity is much lower, and the added active oxides preserve their high dispersion. It is not excluded that the lower porosity of impregnated catalysts, in particular granulated, compared to the porosity of kneaded catalysts results in a decrease in the activity.

Comparative test data obtained with α-Fe_2O_3-based catalysts modified with CuO (Co_3O_4) and traditional complete oxidation catalysts (IC-12-1, ICT-12-6, MPB-PC) for the reaction of butane oxidation processes demonstrate that the former reveal a higher activity and thermal stability, even at a lower concentration of the active components. The high activity of iron-chromium catalysts (samples No. 8–10) to butane oxidation should be mentioned, therefore they can be recommended for oxidation of hydrocarbons. Unfortunately, they are not active to oxidation of CO: the conversion equal to 25 % under standard test conditions is attained at *ca.* 320 °C over the granulated catalyst.

A monolithic perovskite-containing catalyst has been prepared by addition of mixed perovskite-containing oxide $LnMnO_3$ (in amount of 10 %) at the stage of plastic paste preparation from Fe_2O_3-(Cl) with HATCA used as binder and HNO_3 (or CH_3COOH) as electrolyte. The catalyst can be used both for low-temperature and high-temperature oxidation processes (sample No. 11). The activity of this catalyst for oxidation of butane is not lower than that of copper oxide or cobalt oxide catalyst. Again, it is active in CO oxidation: The conversion equal to 25 % is attained at *ca.* 150 °C over the granulated catalyst.

CONCLUSION

Inexpensive, active and stable catalysts of various shapes for complete oxidation processes have been developed based on iron oxides of different origins, including the cheapest feedstock supplied by the Novokuznetsk Metallurgical Plant. Properties of iron oxide based catalysts and supports depend on the preparation conditions including the nature of the feedstock, application of mechanochemical treatment, nature of electrolyte, binder *etc*. Regularities of formation of the catalyst texture have been determined.

REFERENCES

1 A. S. Ivanova, V. V. Pugach, E. M. Moroz and I. A. Ovsyannikova, *Kinetika i kataliz*, 28 (1987) 1424.

2 A. S. Ivanova, V. V. Pugach, E. M. Moroz and I. A. Ovsyannikova, *Ibid*., 30 (1989) 1160.

3 S. Scire, S. Minico, C. Crisafulli and S. Galvagno, *Catal. Commun*., 2 (2001) 229.

4 L. A. Isupova, V. Yu. Aleksandrov and V. V. Popovskii, Proc. 5 Intern. Conf. “Kataliticheskaya ochistka gazov”, Tbilisi, 1989, pp. 3–5 (in Russian).

5 L. A. Isupova, V. Yu. Aleksandrov, V. V. Popovskii *et al*., *Zhurn. prikl. khimii*, 9 (1988) 1976.

6 W. M. Carty and P. W. Lednor, Current Orinion in Solid State and Mater. Sci., vol. 1, 1996, pp. 88–95.

7 L. A. Isupova, G. M. Alikina, O. I. Snegurenko *et al*., *Appl. Catal. B: Environm*., 21 (1999) 171.

8 A. S. Lisitsyn, A. V. Golovin, V. L. Kuznetsov and Yu. I. Ermakov, *J. Catal*., 95 (1985) 527.

9 T. Alen, Partical Size Measurement, Capt. Hill, London, 1981.

10 V. A. Razdobarov, Influence of Defects on the Catalytic Activity of Spinel and Corundum Type Oxides in CO Oxidation Process, Ph. D. thesis, Boreskov Institute of Catalysis, Novosibirsk, 1992 (in Russian).

11 A. C. Oliveira, A. Valentini, P. S. S. Norbe and M. C. Rangel, *React. Kinet. Catal. Lett*., 75 (2002) 135.

12 N. V. Dvoretskii and L. G. Alikanova, *Khimiya i khimicheskaya tehnologiya*, 45 (2002) 149.

13 V. A. Sadykov, L. A. Isupova, S. V. Tsybulya *et al*., *J. Solid State Chem*., 123 (1996) 191.

14 L. A. Isupova, V. Yu. Aleksandrov, V. V. Popovskii *et al*., *React. Kinet. Catal. Lett*., 31 (1986) 195.

15 S. F. Tikhov, V. A. Sadykov, G. N. Kryukova *et al*., *J. Catal*., 134 (1992) 506.